行政院國家科學委員會專題研究計畫成果報告

以任意力理論分析具揮發性液滴之馬崙葛尼不穩定性

計畫類別：☑個別型計畫　　□整合型計畫
計畫編號：NSC89-2212-E-002-138
執行期間：89年8月1日至90年7月31日

計畫主持人：賴君亮

本成果報告包括以下應繳交之附件：
- □赴國外出差或研習心得報告一份
- □赴大陸地區出差或研習心得報告一份
- □出席國際學術會議心得報告及發表之論文各一份
- □國際合作研究計畫國外研究報告書一份

執行單位：國立台灣大學工學院機械工程學系

中華民國九十年七月三十一日

誌 謝

本研究計畫在中華民國國家科學委員會的贊助下得以順利完成，特此深致謝意。

中文摘要

以任意力理論分析具揮發性液滴之馬崙葛尼不穩定性

暫態基本場的穩定性分析是比較困難的。因為任何存在於系統中的擾動，其隨時間的變化情形，將與不斷改變中的基本場產生關聯，彼此互為影響。況且，針對暫態基本場的穩定性分析，目前仍未能提出通用的判斷準則。鑑於此，本研究擬利用任意力理論來分析暫態基本場的穩定性。期盼以統計學的觀點來描述一直不間斷被引入系統中的擾動波，使所得的統御方程組，更能真實地呈現持續變化的基本場與成長中的擾動波之間的關聯性，以及顯明馬崙葛尼數和隨意引入系統中的擾動波，對整個系統穩定性的影響。再者，本研究將以探討具揮發性的液滴之馬崙葛尼不穩定現象為例，仔細地比較先前學者以不同的穩定性分析方法，在不穩定現象發生的預測上有否差異。歸納所得，對相關的現象，彼此都有類似的預測。唯因缺乏具體的實驗數據供作參考；故此，未能就此推論何種分析方法相對地比較優越。然而，這些不同的分析方法都對瞭解系統的不穩定現象提供了多方面寶貴的訊息。

Abstract

Theoretical Analysis of Marangoni Instability of an Evaporating Droplet by Random Forcing Theory

The stability analysis for a time-dependent flow is difficult because the disturbances are continually interacting with the basic flow field which itself is evolving with time. In addition, there still exists no universal instability criterion. In order to simulate the constantly introduced disturbances and its interaction with the basic flow field, the random forcing theory with a stochastic formulation is applied to analyze the onset of Marangoni instability of an evaporating droplet. Results from the previous studies are included for comparison. It is indicated that similar trends for the onset of instability are predicted by different methods which include the linear stability analysis with a frozen temperature profile, the energy method, the initial-value technique, and the random forcing theory. However, due to the lack of experimental data, it is hard to decide at this moment which method is the most appropriate one. Nevertheless, they are all in some way helpful in understanding the physical mechanism and the onset of the Marangoni instability of an evaporating droplet.

Contents

List of Tables

List of Figures

List of Symbols

Bi	heat exchange parameter
Cr	Crispation number
D	mass diffusivity
D_1	the rate of viscous dissipation
D_2	the work done by Marangoni forces acting on the droplet surface
D_3	the work done by random forces
E_{kin}	disturbance kinetic energy
Ev	dimensionless evaporation rate
$\mathbf{F}$	a function arising due to the random stress tensor (referred to equation (3.4))
$\mathbf{f}$	random forcing function given by equation (3.10)
h_{lg}	latent heat of evaporation
k	thermal conductivity
L^2	operator
l	wave number of the disturbances
M_{amb}	molecular weight of air
M_l	molecular weight of the evaporating liquid
M_s	the smallest mean Nusselt number the measuring instrument could detect (referred to the work of Jhaveri & Homsy [36],[37])
Ma	Marangoni number
m	azimuthal wave number
m'	dimensional evaporation rate
m_v	mole fraction of liquid vapor
P_l^m	associated Legendre polynomials
Pr	Prandtl number
p	pressure
p_1	the pressure work done by perturbed field

Q	dimensionless heat flux due to the evaporation
$\mathbf{q}'$	random heat flux vector
q'	components of the random heat flux vector
R, θ, ϕ	dimensionless spherical coordinates
$\dot{R}$	regression rate of the evaporating free surface
r, θ, ϕ	dimensional spherical coordinates
r_0	radius of the evaporating droplet
r_w	ratio of molecular weights M_{amb}/M_l
$\mathbf{S}'$	random stress tensor
S'	components of the random stress tensor
T	temperature
t	dimensional time
U	magnitude of the perturbed R-component velocity
u	velocity component
$\vec{V}$	velocity vector
Y	mass fraction of the liquid vapor
Y_l^m	spherical harmonics

Greek Symbols

α	thermal diffusivity
δ_1	one dimensional delta function
δ_3	three dimensional delta function
ϵ_{12}	Lennard-Jones force constant
μ	viscosity
ν	kinematic viscosity
ρ	density
σ	surface tension
σ_{12}	Lennard-Jones force constant
τ	dimensionless time
Φ	variance of the random forcing function
Φ_1	variance of the random stress tensor

Φ_1 variance of the random heat flux vector

ϕ_k thermal conductivity ratio

ϕ_α thermal diffusivity ratio

ϕ_μ viscosity ratio

ϕ_ρ density ratio

χ defined parameter indicating the heat transfer due to temperature perturbation

Ω_D collision integral for mass diffusion

Miscellaneous Symbols

$\Re$ universal gas constant

$\Im$ magnitude of temperature perturbation

Superscripts

$'$ perturbed quantity

$*$ dimensionless quantity

Subscripts

b boiling state

c critical condition

g gas property

l liquid property

v vapor property (of the evaporating liquid)

ref reference state

s surface condition

0 initial condition

∞ far field

Chapter 1

Introduction

1.1 BACKGROUND

The stability of fluid systems in a transient basic state is a very complicated phenomenon. There exists strong coupling between the transient basic state and the perturbed fields. Hence, not only the criterion for the onset of instability but also the onset time is crucial to such a transient problem.

Most theoretical works on the determination of the onset time of the instability of a time-dependent flow can be classified into three categories, namely, the method of "frozen" time, the energy method, and the method using initial-value technique. The first method is to obtain the marginal stability by freezing the diffusing basic state at a specific time of interest ([1], [5], [18], [26], [27], [67]). The energy method can determine the lower bound of the onset time ([15], [16], [17], [25], [32], [33], [38], [39], [40], [41], [51], [52], [60]). These methods can predict the onset time of convection without any arbitrariness since the time appears only parametrically, but the calculated onset time is, in general, considerably lower than the experimental observations. The initial-value technique was introduced by Foster [21] and investigated afterwards by other researchers ([10], [24], [48]). With suitably chosen initial disturbances and amplification factors, the onset time predicted by this method agrees well with that measured. However, the results show a marked sensitivity to the initial data [24] and, to fit the experiments, amplification factors ranging over several orders are necessary. Another theoretical weakness of the initial-value approach lies in the assumption that the disturbances are present only at the initial instant.

In an actual laboratory experiment, disturbances of unknown amplitudes resulting

from several disturbances sources (e.g., vibration, roughness, unevenness in heating, etc.) are always present. It is unlikely to have identical initial disturbances in two experimental runs. Some investigations ([4], [22], [48], [53]) regarding the experimental determination of the onset time have been reported, indicating that when the same experimental run was carried out in two different apparatuses, no substantial difference in the measurements of the onset time was found. Thus it was suggested that the initial disturbances had no effect on the onset time and all evolutions in an experiment were statistically correlated so as to have reproducible average transport. Moreover, they might have evolved from a statistical distribution of the initial disturbances. In light of these observations, it seems appropriate to develop a model in which the random nature of the disturbances is treated statistically.

At the earlier stage, the study of random convection problems was mainly on the effects of the randomly chosen initial conditions. With the controlled and uncontrolled initial conditions, the effects of the random noise on the onset of fluctuating flow in a layer heated from below have been examined experimentally [7] and theoretically [6]. Because of the existence of several possible static solutions, the randomness in the initial conditions and the small imperfections became amplified and would not be so easy to die away as in the case when the static solution was unique. Small amounts of noise in the initial conditions would cause continuous variations of the flow pattern. Although they did not dominate the development of the convection pattern exclusively, they tended to obscure qualitatively the differences in the convection flows in different parametric ranges of the system. Similar results regarding the stability of the convective flow in a cubic box of fluid-saturated porous material heated from below have been reported by Straus & Schubert [64] and by Horne [34]. The flow pattern at a particular value of Rayleigh number was not unique and was determined by the initial conditions (randomly chosen). They led to either steady two-dimensional or steady three-dimensional convection. In view of the indeterminacy of the final steady-state configuration, the authors suggested that, if a sufficient number of numerical calculations was taken, it would be possible to characterize, from a probabilistic point of view, the set of random initial conditions leading to a particular form of convection.

Furthermore, a random force term has been added to the governing equations with the consideration of the continuous presence of noise during the evolution of instability. By adding the Gaussian white noise to a dynamical system, Ludwig [46] has

shown that a system, at an asymptotically stable equilibrium state, would eventually lose its stability with the influence of random effects. The persistence of the system, which was referred as the expected time elapsed before leaving its stable state, could be evaluated approximately by means of the asymptotic solution of the resulting diffusion equation when the strength of the noise was small. Including the random-force terms suggested by Landau and Lifshitz [44], Zaitsev & Shliomis [70] and Graham [23] studied the hydrodynamic fluctuations near the critical Rayleigh number of a liquid heated from below with different boundary conditions. The velocity and temperature fluctuations increased strongly when the critical Rayleigh number was approached, and their time-dependent correction functions were also obtained. Later, the onset of Rayleigh-Benard convection was reconsidered by Jhaveri & Homsy [36]. By introducing the thermodynamically determined fluctuating forces into the governing equations, they tried to describe the time evolution of a periodic solution (two-dimensional rolls in horizontal direction) to an ordered convection. An ensemble mean Nusselt number was calculated from N independent sample realizations. Three stages in the evolution of an ordered convection from random fluctuations were identified and discussed.

Following their earlier work, Jhaveri & Homsy [37] then solved the randomly forced initial value problem numerically at high Rayleigh numbers for both the cases with a step change and a temporally linear increase in surface temperature. The onset time was defined as the time at which the mean Nusselt number first reached the value M_s, which corresponded to the smallest value of mean Nusselt number. The wave number at the onset of convection was still considered to be the fastest growing one. Excellent agreements were found between the analysis and the experiment. Kim *et al.* ([42], [43]) considered a similar case, where an initially isothermal fluid layer confined by two rigid horizontal surfaces was suddenly heated from blow with a constant heat flux. The dependency of the onset time (defined as the ensemble mean of the time at which the bottom-surface temperature started to decrease for the first time) on the heat flux and the effects of Prandtl number and Rayleigh number were examined; the results agreed quantitatively well with the experimental data. Motivated by the works of Jhaveri & Homsy, Chen *et al.* [9] performed numerical calculations on the stability of an unsteady circular Couette flow with random-force effect. Compared with previous theoretical works, the results showed significantly improved agreement with the experiment.

In order to consider the effects of continually imposed, random disturbances in a stability study of unsteady flows, the random-force theory is employed in the present study to seek the onset time of instability of an evaporating droplet. The mechanism for the onset of instability induced by the surface tension in an evaporating liquid is similar to that of the classical Marangoni instability. A condition of constant heat flux from the free surface is usually used to model the evaporation. Since the temperature distribution in the liquid phase is destabilizing, the system will become unstable under certain circumstances. Many studies have been made to analyze the instability of a planar liquid layer suddenly cooled from above or heated from below ([2], [3], [15], [26], [27], [32], [33], [51], [52], [54], [55], [58], [59], [61], [63], [65], [66], [68], [71]). Much less work has been done on the onset of Marangoni instability in a spherical geometry.

With a constant heat and mass flux, the instability of a deformable spherical droplet suspended in another immiscible liquid was investigated by Sorensen *et al.* [62] using linear stability analysis. In recent years, Pirotte & Lebon [56] analyzed the Marangoni instability of a spherical liquid layer with an undeformable free surface. The critical Marangoni number obtained was higher than that of the planar case [54]. They suggested that it was mainly due to the existence of surface curvature. Investigations were also focused on the problem of instability in a spherical liquid layer with a non-deformable or deformable free surface ([11], [12], [29], [30],[31]). A review of recent work concerning the Marangoni instability in spherical geometry can be found in the research by Lebon, Dauby and Cloot [45]. Wilson [69] extended the earlier work of Pirotte & Lebon [56] to include the effect of a deformable free surface. Ha [26] and Ha & Lai [27] modeled a configuration similar to that of Wilson. The effect of phase change during the evaporation process was considered by simultaneously solving the energy and species equations. With the quasi-steady assumption, the sufficient conditions for the onset of Marangoni instability of an evaporating droplet were determined. The results indicated that, for a non-deformable droplet, both the critical Marangoni number and the critical wave number increased with the initial temperature and decreased with time. Generally, surface deformation is a destabilizing factor. Later, Ha [28] solved the same problem by energy method. Results were in accord with her previous work. In addition to the estimation of the onset time of Marangoni instability of an evaporating droplet with initial-value techniques, Chou [10] further illustrated the physical mechanism of the instability

by analyzing the linear energy balance of the onset mode.

In the above studies, disturbances are present only at the initial instant. Such a classical approach of examining the fate of disturbances introduced at some initial time seems unrealistic. Therefore, it is of interest to model more appropriately the effects of these ever present disturbances by introducing the random-force terms.

1.2 OBJECTIVES OF THE RESEARCH

The aim of the present study is to simulate the situations close to the laboratory experiments by investigating the stability of an evaporating droplet with the inclusion of continually imposed random disturbances. Firstly, the governing equations of the system are derived. The stability criterion are then obtained. Comparison with the results obtained previously will be discussed finally.

The basic assumptions and the corresponding mathematical formulation for an evaporating droplet are described in Chapter 2. In Chapter 3, the onset time of the Marangoni instability of an evaporating droplet is obtained and the results are presented and discussed. Finally, conclusions from the present study and the future work will be given in Chapter 4.

Chapter 2

Mathematical Formulation

Evaporation at the surface of a liquid is an unsteady process involving heat and mass transport. The process of evaporation also leads to a local reduction in the temperature of the bulk liquid near the surface. Marangoni instability may then be induced by such a surface temperature reduction and the consequent variation in surface tension.

General descriptions of the onset of Marangoni instability of an evaporating droplet can be referred to Ha [26] and Ha & Lai [27]. Attention is paid specifically to the evaporation of a quiescent droplet. The mathematical formulation and the criterion of the onset of instability will be given in the following.

2.1 THE GOVERNING EQUATIONS AND BOUNDARY CONDITIONS

The physical system consists of a motionless droplet of radius r_0, surrounded by a passive gas with an initial mass fraction Y_∞ of the evaporating component and at temperature T_0 and pressure p_∞. The droplet is originally at pressure p_0 and the same initial temperature T_0 as the surrounding gas. A schematic diagram of the physical model is depicted in figure 2.1.

Strictly speaking, evaporation is never a steady process since the position of the free surface is changing and the surface temperature and evaporation rate keep decreasing during evaporation. However, by comparing the time scales of the gas phase and the interface regression (referred to table 2.1) with the time scale of the heat diffusion in the liquid phase, the gas phase (the surrounding air) can be treated

as asymptotically steady and the position change of the interface is negligible in this study. This approximation will become more reasonable by choosing a material with a higher density ratio between the liquid phase and its vapor and a larger size of droplet.

To addition, all physical properties of the fluid except the surface tension, which is linearly dependent on temperature, are assumed constant. Throughout the work, the gravity effect, viscous dissipation and radiative heat transfer will be neglected. The free surface is undeformable and both the liquid and gas phases are assumed incompressible.

With these basic assumptions and by introducing the following dimensionless variables

$$R = \frac{r}{r_0} \ , \quad \vec{V}^* = \frac{\vec{V}}{\alpha_l / r_0} \ , \quad \tau = \frac{t}{r_0^2/\alpha_l} \ ,$$
$$T^* = \frac{T}{m_0' h_{lg} r_o / k_l} \ , \quad p^* = \frac{p}{\rho_l \alpha_l^2 / r_0^2} \ , \quad Y^* = \frac{Y}{Y_0} \ , \tag{2.1}$$

the dimensionless governing equations for the flow, which take the same form as in a previous study by Ha [26], are

$$\nabla \cdot \vec{V}_g^* = 0, \tag{2.2}$$
$$\nabla \cdot \vec{V}_l^* = 0, \tag{2.3}$$
$$\frac{\phi_\alpha}{Pr_g}\left(\vec{V}_g^* \cdot \nabla \vec{V}_g^* + \phi_\rho \nabla p_g^*\right) = \nabla^2 \vec{V}_g^*, \tag{2.4}$$
$$\frac{1}{Pr_l}\left(\frac{\partial \vec{V}_l^*}{\partial \tau} + \vec{V}_l^* \cdot \nabla \vec{V}_l^* + \nabla p_l *\right) = \nabla^2 \vec{V}_l^*, \tag{2.5}$$
$$\phi_\alpha \left(\vec{V}_g^* \cdot \nabla T_g^*\right) = \nabla^2 T_g^*, \tag{2.6}$$
$$\frac{\partial T_l^*}{\partial \tau} + \vec{V}_l^* \cdot \nabla T_l^* = \nabla^2 T_l^*, \tag{2.7}$$
$$\phi_\alpha Le \left(\vec{V}_g^* \cdot \nabla Y_v^*\right) = \nabla^2 Y_v^*. \tag{2.8}$$

In the above equations, $\vec{V}$ is the velocity vector; T is the temperature; p denotes the pressure and τ is time. Y_v is the mass fraction of the liquid vapor and Y_0 is its initial value at the droplet surface. $\phi_\alpha = \frac{\alpha_l}{\alpha_g}$ is the thermal diffusivity ratio and $\phi_\rho = \frac{\rho_l}{\rho_g}$ is the density ratio. $Pr = \frac{\nu}{\alpha}$ is the Prandtl number and $Le = \frac{\alpha}{D}$ is the Lewis number. Subscripts g and l refer to the gas phase and liquid phase, respectively, and superscript $*$ indicates that the physical quantity is dimensionless.

The initial conditions, $\tau = 0$, are

$$\vec{V}_l^* = 0, \quad T_l^* = 0. \tag{2.9, 2.10}$$

As $R \to \infty$, the solutions must satisfy

$$\vec{V}_g^* = 0, \qquad T_g^* = 0, \tag{2.11, 2.12}$$

$$p_g^* = p_\infty^*, \qquad Y_v^* = Y_\infty^* = 0. \tag{2.13, 2.14}$$

At the center of the droplet, $R = 0$, the boundary conditions are

$$\vec{V}_l^* = 0, \quad T_l^* = \text{finite}. \tag{2.15, 2.16}$$

At the droplet surface, $R = 1$, the continuity of velocity, mass flux, temperature and heat flux, the non-condensible condition of the passive gas and the balance of forces must be satisfied. They are expressed as follows.

$$u_{\theta,l}^* = u_{\theta,g}^*; \quad u_{\phi,l}^* = u_{\phi,g}^*, \tag{2.17, 2.18}$$

$$u_{R,l}^* - \dot{R} = \frac{1}{\phi_\rho}(u_{R,g}^* - \dot{R}) = Ev, \tag{2.19}$$

$$T_g^* = T_l^* = T_s^*, \tag{2.20}$$

$$-\frac{\partial T_l^*}{\partial R} = -\frac{1}{\phi_k}\frac{\partial T_g^*}{\partial R} + \frac{m'}{m_0'}, \tag{2.21}$$

$$\frac{1}{\phi_\alpha Le}\frac{\partial Y_v^*}{\partial R} = -\Big(\frac{1}{Y_0} - Y_v^*\Big)u_{R,g}^*, \tag{2.22}$$

$$\begin{aligned} -\phi_\mu\Big[R\frac{\partial}{\partial R}\Big(\frac{u_{\theta,l}^*}{R}\Big) + \frac{1}{R}\frac{\partial u_{R,l}^*}{\partial \theta}\Big] + \Big[R\frac{\partial}{\partial R}\Big(\frac{u_{\theta,g}^*}{R}\Big) &+ \frac{1}{R}\frac{\partial u_{R,g}^*}{\partial \theta}\Big] \\ &= \frac{\phi_\mu Ma}{R}\frac{\partial T^*}{\partial \theta}, \end{aligned} \tag{2.23}$$

$$\begin{aligned} -\phi_\mu\Big[\frac{1}{R\sin\theta}\frac{\partial u_{R,l}^*}{\partial \phi} + R\frac{\partial}{\partial R}\Big(\frac{u_{\phi,l}^*}{R}\Big)\Big] + \Big[\frac{1}{R\sin\theta}\frac{\partial u_{R,g}^*}{\partial \phi} &+ R\frac{\partial}{\partial R}\Big(\frac{u_{\phi,g}^*}{R}\Big)\Big] \\ &= \frac{\phi_\mu Ma}{R\sin\theta}\frac{\partial T^*}{\partial \phi}, \end{aligned} \tag{2.24}$$

$$\left(-p_l^* + 2Pr_l\frac{\partial u_{R,l}^*}{\partial R}\right) - \left(-p_g^* + \frac{2Pr_g}{\phi_\alpha\phi_\rho}\frac{\partial u_{R,g}^*}{\partial R}\right) = -2\frac{Pr_l}{Cr}, \tag{2.25}$$

where $\phi_k = \frac{k_l}{k_g}$ is the heat conductivity ratio and $\phi_\mu = \frac{\mu_l}{\mu_g}$ is the viscosity ratio. $Ev = \frac{m'r_0}{\rho_l\alpha_l}$ is the dimensionless evaporation rate per unit area per unit time at the free surface. The expression for Ev will be obtained later by using the velocity field of the gas phase. $Cr = \frac{\mu_l\alpha_l}{\sigma_0 r_0}$ is the Crispation number with σ_0 being the surface tension at T_0. $Ma = -\frac{(\partial\sigma/\partial T)\ m_0' h_{lg} r_0^2}{\mu_l\alpha_l k_l}$ is the Marangoni number, where m_0' is the initial evaporation rate at the droplet surface and h_{lg} represents the latent heat of evaporation at T_0. $\dot{R}$ is the regression rate of the droplet which will be neglected in the later analysis while is still retained here for the sake of mass balance.

2.2 THE BASIC FLOW

Since the attention is focused on the evaporation of a quiescent droplet, no motion occurs in the liquid phase. The pressure in the droplet is then constant and can be determined by the condition of normal-force balance on the surface, equation (2.25), as follows

$$p_l^* = \frac{2Pr_l}{Cr} - \frac{4Pr_g}{\phi_\alpha^2\phi_\rho Le}\ln(1-Y_v(1)) - \frac{1}{2\phi_\rho\phi_\alpha^2 Le^2}\ln^2(1-Y_v(1)) + p_\infty^*. \tag{2.26}$$

The radial velocity, pressure, temperature, and liquid vapor distribution in the surrounding gas phase can be derived analytically in the following forms from the corresponding equations and boundary conditions.

$$u_{R,g}^* = -\frac{\ln(1-Y_v(1))}{\phi_\alpha Le}\frac{1}{R^2}, \tag{2.27}$$

$$p_g^* = -\frac{\ln^2(1-Y_v(1))}{\phi_\alpha^2\phi_\rho Le^2}\frac{1}{2R^4} + p_\infty^*, \tag{2.28}$$

$$T_g^* = T_s^*\frac{(1-Y_v(1))^{\frac{1}{Le}\frac{1}{R}} - 1}{(1-Y_v(1))^{\frac{1}{Le}} - 1}, \tag{2.29}$$

$$Y_v^* = \frac{1}{Y_0}\left[1-(1-Y_v(1))^{\frac{1}{R}}\right], \tag{2.30}$$

where

$$Y_v(1) = \frac{\exp\left[\frac{h_{fg}}{\Re}\left(\frac{1}{T_b}-\frac{1}{T_s}\right)\right]}{r_w - (r_w-1)\exp\left[\frac{h_{fg}}{\Re}\left(\frac{1}{T_b}-\frac{1}{T_s}\right)\right]}$$

is the mass fraction of liquid vapor at the droplet surface. The dimensionless evaporation rate is then determined by the condition of continuity of mass flux, equation (2.19), i.e.,

$$Ev = -\frac{1}{Le\phi_a(\phi_\rho - 1)} \ln(1 - Y_v(1)). \tag{2.31}$$

The temperature field of the droplet, $T_l^*(R, \tau)$, can not be solved easily in an analytic form and has to be determined from the following energy equation and conditions:

$$\frac{\partial T_l^*}{\partial \tau} = \frac{1}{R^2}\frac{\partial}{\partial R}(R^2 \frac{\partial T_l^*}{\partial R}), \tag{2.32}$$

$$\tau = 0, \qquad T_l^* = 0, \tag{2.33}$$

$$R = 0, \qquad T_l^* = \text{finite}, \tag{2.34}$$

$$R = 1, \qquad -\frac{\partial T_l^*}{\partial R} = T_s^* Bi + Q. \tag{2.35}$$

In equation (2.35), the first term of the right hand side represents the heat transfer to the ambient by convection and the second term denotes the heat flux due to evaporation at the free surface, with the parameters defined as

$$Bi = \frac{1}{\phi_k Le} \ln(1 - Y_v(1)) \frac{(1 - Y_v(1))^{\frac{1}{Le}}}{(1 - Y_v(1))^{\frac{1}{Le}} - 1}, \tag{2.36}$$

$$Q = \frac{m'}{m_0'} = \frac{\ln(1 - Y_v(1))}{\ln(1 - Y_0(1))}. \tag{2.37}$$

2.3 THE STOCHASTIC FORMULATION

It is the purpose of this work to develop a simple but more realistic theoretical model to predict the onset of the instability of an evaporating droplet. Generally, the random force due to the continually imposed random fluctuations can be considered to be a stochastic variable with a specified probability distribution. The most basic mode is the molecular thermal fluctuations, which can be represented by a Gaussian white noise [44]. In order to demonstrate the analysis as mathematically simple as possible, only a Gaussian distribution of the infinitesimally small fluctuations within

the droplet is assumed. Hence, the linearized dimensionless equations (of the liquid phase) for the fluctuating quantities, are as follows

$$\nabla \cdot \vec{V}' = 0, \tag{2.38}$$

$$\frac{1}{Pr}\left(\frac{\partial \vec{V}'}{\partial \tau} + \nabla p'\right) = \nabla^2 \vec{V}' + \nabla \cdot \mathbf{S}', \tag{2.39}$$

$$\frac{\partial T'}{\partial \tau} + \vec{V}' \cdot \nabla T^* = \nabla^2 T' + \nabla \mathbf{q}'. \tag{2.40}$$

The effect on the Marangoni instability of an evaporating droplet due to the surrounding atmosphere is directly determined by the thermal and mass boundary conditions on the interface (shown later). The superscript "$\prime$" is used here to denote the disturbances while l, used for the liquid phase previously, is omitted for simplification. $\mathbf{S}'$ and $\mathbf{q}'$ are, respectively, the Gaussian random stress tensor and Gaussian random heat-flux vector. The statistical corrections of the dimensionless random quantities are given as follows:

$$< \mathbf{S}' > = 0, \tag{2.41}$$

$$< \mathbf{q}' > = 0, \tag{2.42}$$

$$< S_1'(R_1, \tau_1)\, S_2'(R_2, \tau_2) > = \Phi_1 \delta_3(R_1 - R_2)\delta_1(\tau_1 - \tau_2), \tag{2.43}$$

$$< q_1' q_2' > = \Phi_2 \delta_3(R_1 - R_2)\delta_1(\tau_1 - \tau_2), \tag{2.44}$$

$$< S_{jk}' q_i' > = 0, \tag{2.45}$$

with Φ_1 and Φ_2 being the variance of the random stress tensor and the random heat flux vector respectively. δ_3 and δ_1 are the three dimensional and one dimensional delta functions. Usually, Φ_2 is a much smaller parameter compared with Φ_1 for most fluids ([36], [42]), and so $\mathbf{q}'$ can be neglected in what follows.

The boundary conditions at the center of the droplet are

$$\vec{V}',\ T' = \text{finite}. \tag{2.46, 2.47}$$

On the free surface, the boundary conditions are

$$u_R' = \frac{\partial Ev}{\partial T^*} T', \tag{2.48}$$

$$R\frac{\partial}{\partial R}(\frac{u'_\theta}{R}) + \frac{1}{R}\frac{\partial u'_R}{\partial \theta} = -\frac{Ma}{R}\frac{\partial T'}{\partial \theta}, \tag{2.49}$$

$$\frac{1}{R\sin\theta}\frac{\partial u'_R}{\partial \phi} + R\frac{\partial}{\partial R}(\frac{u'_\phi}{R}) = -\frac{Ma}{R\sin\theta}\frac{\partial T'}{\partial \phi}, \tag{2.50}$$

$$-p' + 2Pr\frac{\partial u'_R}{\partial R} = \frac{2}{R}PrMaT', \tag{2.51}$$

$$-\frac{\partial T'}{\partial R} = (Bi + \frac{\partial Bi}{\partial T^*}T^* + \frac{\partial Q}{\partial T^*})T', \\ = \chi T'. \tag{2.52}$$

Equations (2.38)-(2.52) are solved numerically to find the onset mode of the Marangoni instability of an evaporating droplet.

2.4 THE DISTURBANCE KINETIC ENERGY EQUATION

One difficulty encountered in the stability analysis of a time-dependent flow is that there is no obvious definition of instability. To detect the onset of convection, some statistical mean value properties of the ensemble are chosen for representing the evolution of disturbances. To evaluate the onset time, Jhaveri & Homsy ([36], [37]) have defined the onset time as the time at which the ensemble mean Nusselt number reached a prescribed number M_s. The value $M_s(> 1)$ corresponds to the smallest mean Nusselt number the measuring instrument could detect. Kim *et al.* ([42], [43]) introduced a modified Nusselt number whose value started to grow at the onset time. Chen *et al.* [9] determined the onset of instability by measuring the departure of the axial velocity from a nonzero mean velocity, which was computed by averaging the axial velocity over the time interval of interest. However, in the present study, the growth characteristics of the disturbance kinetic energy is chosen for the determination of the onset of Marangoni instability of an evaporating droplet.

First, consider the mechanism of the classical Marangoni convection as described by Pearson [54]. The physical system is a static liquid layer heated from below. When a hot spot appears on the interface as a result of some random temperature disturbances, the resultant thermocapillary stresses generate a surface flow away from the spot in all directions. Conservation of mass is then satisfied by a vertical upflow underneath the spot. Since the temperature of the fluid increases downward from the interface, this upflow heats up the spot. If the vertical temperature gradient in the layer is large enough, the convective heating will overcome the cooling effects

of conduction and the temperature of the surface hot spot will increase. The system is then unstable. Hence, energy being continually extracted from the basic-state temperature field to the perturbed field is a good indication for the occurrence of convection. A similar situation is involved in the onset of the Marangoni instability of an evaporating droplet. Therefore, the energy transfer between the basic state and the perturbed field would be an appropriate criterion to determine the onset time of instability. In the present study, the onset time of instability is defined as the time at which the disturbance kinetic energy is equal to or greater than 1000 times of its initial value as suggested by Chen *et al.* [8].

By taking the dot product of equation (2.39) with $\vec{V}'$ and, then, integrating over the whole droplet with the aid of the continuity equation (2.38), the equation determining the rate of change of the kinetic energy, E_{kin}, is derived:

$$\begin{aligned}\frac{1}{Pr}\frac{dE_{kin}}{d\tau} &= \frac{1}{Pr}\frac{d}{d\tau}\ll\frac{|\vec{V}'|^2}{2}\gg = -\frac{1}{Pr}\ll\nabla\cdot(\vec{V}'p')\gg + \ll\nabla\cdot(\vec{V}'\times\nabla\times\vec{V}')\gg \\ &\quad - \ll(\nabla\times\vec{V}')\cdot(\nabla\times\vec{V}')\gg \\ &\quad - \ll\vec{V}'\cdot(\nabla\cdot\mathbf{S}')\gg, \qquad (2.53)\end{aligned}$$

where $\ll\ \gg$ denotes the volume integration over the whole droplet. Taking into account the boundary conditions and using Green's theorem, the rate of change of the kinetic energy can be written as

$$\frac{1}{Pr}\frac{dE_{kin}}{d\tau} = p_1 + D_1 + D_2 + D_3. \qquad (2.54)$$

In the above expression, p_1 denotes the pressure work done by perturbed field, i.e.,

$$\begin{aligned}p_1 &= -\frac{1}{Pr}\ll\nabla\cdot(\vec{V}'p')\gg, \\ &= -2\int_S(u'_R\frac{\partial u'_R}{\partial R})dS + 2Ma\int_S u'_R\frac{T'}{R}dS. \qquad (2.55)\end{aligned}$$

where p' has been replaced by equation (2.51) and symbol S denotes the evaporating surface of the droplet. D_1 is the rate of viscous dissipation

$$D_1 = - \ll (\nabla \times \vec{V}') \cdot (\nabla \times \vec{V}') \gg + 2 \int_S \Big(\frac{{u'_\theta}^2}{R} - \frac{u'_\theta}{R} \frac{\partial u'_R}{\partial \theta} + \frac{{u'_\phi}^2}{R} - \frac{u'_\phi}{R \sin\theta} \frac{\partial u'_R}{\partial \phi} \Big) dS. \tag{2.56}$$

D_2 is the work done by Marangoni forces acting on the droplet surface in the latitudinal and azimuthal directions

$$D_2 = -Ma \int_S \Big(\frac{u'_\theta}{R} \frac{\partial T'}{\partial \theta} + \frac{u'_\phi}{R \sin\theta} \frac{\partial T'}{\partial \phi} \Big) dS, \tag{2.57}$$

and D_3 is the work done by random forces

$$D_3 = \ll \vec{V}' \cdot (\nabla \cdot \mathbf{S}') \gg . \tag{2.58}$$

Details of the derivation can be referred to the work of Chou [10]; besides, the random-force terms have to be included in the momentum equation.

The disturbance kinetic energy equation (2.53) must be exactly satisfied by any solution of the linearized stability problem. If the rate of change of kinetic energy is positive ($\partial_t E_{kin} > 0$), the basic flow is unstable. Therefore, terms on the right hand side of equation (2.53) with a positive (negative) sign are destabilizing (stabilizing).

Sine D_1 is negative, referring to the results of Chou [10], it is stabilizing. However, the sign and the magnitude of D_3 depend sensitively on both the form of the onset mode of instability and the random forces. Unlike D_3, the work done by surface forces (D_2) and pressure (p_1) depends solely on the perturbation solutions of equations (2.38) - (2.40) on the surface.

Therefore, the numerical calculations of the perturbed fields and the disturbance kinetic energy are presented in next chapter. The the onset time of instability is then determined by investigating the time evolution of the disturbance kinetic energy.

Chapter 3

Numerical Simulation

The random fluctuations in an evaporating droplet are taken into account as a Gaussian white noise source, by adding the fluctuating δ-correlated force. With observation of the growth characteristics of the disturbance kinetic energy, the onset time of Marangoni instability of an evaporating droplet can be obtained. In the following, the random fluctuating problem, equations (2.38) - (2.52), and its disturbance kinetic energy (2.53) are solved numerically. The results are then discussed and compared with that obtained by the other theoretical works ([26], [27], [28], [10])).

3.1 SOLUTION PROCEDURE

By virtue of the continuity equation, the two tangential stress boundary conditions, equations (2.49) & (2.50), can be combined into a single one (see Appendix A):

$$\frac{\partial^2}{\partial R^2}(Ru'_R) - \frac{(2+L^2)(Ru'_R)}{R^2} = \frac{Ma}{R}L^2T', \tag{3.1}$$

where

$$\begin{aligned} L^2 &= \frac{1}{\sin\theta}\frac{\partial}{\partial\theta}(\sin\theta\frac{\partial}{\partial\theta}) + \frac{1}{\sin^2\theta}\frac{\partial^2}{\partial\phi^2}, \\ &= R^2\nabla^2 - \frac{\partial}{\partial R}(R^2\frac{\partial}{\partial R}), \end{aligned} \tag{3.2}$$

with ∇^2 denoting the Laplace operator in the spherical coordinates, i.e.,

$$\nabla^2 = \frac{1}{R^2}\frac{\partial}{\partial R}(R^2\frac{\partial}{\partial R}) + \frac{1}{R^2\sin\theta}\frac{\partial}{\partial\theta}(\sin\theta\frac{\partial}{\partial\theta}) + \frac{1}{R^2\sin^2\theta}\frac{\partial^2}{\partial\phi^2}. \tag{3.3}$$

By eliminating the pressure term in equation (2.39), the perturbed R-momentum equation in terms of u'_R can be derived as follows (see Appendix B):

$$(\nabla^2 - \frac{1}{Pr}\frac{\partial}{\partial \tau})\nabla^2(Ru'_R) = \mathbf{F}, \tag{3.4}$$

where $\mathbf{F} = \vec{R} \cdot \nabla \times \nabla \times \nabla \cdot \mathbf{S}'$ arises due to the random stress tensor.

Motivated by the operator L^2, the spatial dependence of the fluctuating flow can be simplified and the random dependent variables are represented as spherical harmonics components with random time-dependent amplitudes, i.e.,

$$\begin{aligned} Ru'_R &= U(R,\tau)Y_l^m(\theta,\phi), \\ T' &= \Im(R,\tau)Y_l^m(\theta,\phi). \end{aligned} \tag{3.5}$$

The spherical harmonics Y_l^m satisfies the following equation

$$[\frac{1}{\sin\theta}\frac{\partial}{\partial\theta}(\sin\theta\frac{\partial}{\partial\theta}) + \frac{1}{\sin^2\theta}\frac{\partial^2}{\partial\phi^2}]Y_l^m(\theta,\phi) = -l(l+1)Y_l^m(\theta,\phi), \tag{3.6}$$

wherein

$$Y_l^m(\theta,\phi) = P_l^m(\cos\theta)e^{im\phi}, \tag{3.7}$$

and $P_l^m(\cos\theta)$ is the associated Legendre polynomials.

Substituting equation (3.5) into the dimensionless governing equations and boundary conditions and using the orthogonality property of the spatial functions in the fundamental region $(0 \le \phi \le 2\pi, 0 \le \theta \le \pi)$, the following time evolution of the random amplitudes $U(R,\tau)$ and $\Im(R,\tau)$ are obtained, viz.

$$[\frac{d^2}{dR^2} + \frac{2}{R}\frac{d}{dR} - \frac{l(l+1)}{R^2}]\,[\frac{d^2}{dR^2} + \frac{2}{R}\frac{d}{dR} - \frac{l(l+1)}{R^2}]\,U = \mathrm{f}, \tag{3.8}$$

$$[\frac{d^2}{dR^2} + \frac{2}{R}\frac{d}{dR} - \frac{l(l+1)}{R^2}]\,\Im = \frac{U}{R}\frac{\partial T^*}{\partial R}, \tag{3.9}$$

where the random forcing term $\mathrm{f}(R,\tau)$ is

$$\mathrm{f}(R,\tau) = \frac{(2n+1)}{2\pi}\frac{(n-m)!}{(n+m)!}\int_0^{2\pi}\int_0^{\pi} \mathbf{F}\, P_n^m(\cos\theta)\,\cos m\phi\,\sin\theta\, d\theta\, d\phi. \tag{3.10}$$

Moreover, the random forcing function $\mathrm{f}(R,\tau)$ given by the above equation is Gaussian, as is the random shear-stress tensor $\mathbf{S}'$ to which it is linearly related. Its mean and variance satisfy the following relations

$$< \mathrm{f} > \;=\; 0, \tag{3.11}$$

$$< \mathrm{f}(R_1, \tau_1)\mathrm{f}(R_2, \tau_2) > \;=\; \Phi\delta_1(R_1 - R_2)\delta_1(\tau_1 - \tau_2), \tag{3.12}$$

where Φ is equal to 10^{-1}. In fact, the value of Φ should be chosen by referring to the experimental investigations. However, not much quantitative measurements were done for an initially isothermal droplet cooled from its surface due to evaporation. Following the modeling as employed in the work of Chen *et al.* [9], Φ is assigned as 10^{-1} (This value is about 10000 times higher than that associated with thermodynamic fluctuations used in the paper of Jhaveri & Homsy [36] but simulates those fluctuations due to the mechanical vibrations [48].).

At $R = 0$, the following conditions must be satisfied,

$$U = 0; \qquad \Im = \text{finite}. \tag{3.13, 3.14}$$

At $R = 1$, the boundary conditions are

$$\frac{U}{R} \;=\; \frac{\partial Ev}{\partial T^*}\Im, \tag{3.15}$$

$$\frac{d^2U}{dR^2} - \frac{2 - l(l+1)}{R^2}U \;=\; -\frac{Ma}{R}l(l+1)\Im, \tag{3.16}$$

$$-\frac{d\Im}{dR} \;=\; \chi\Im. \tag{3.17}$$

In order to obtain the solutions of the partial differential equations (3.8) and (3.9), it is needed to specify the initial conditions for U and $\Im$. Random initial conditions are considered here. The initial values of U and $\Im$ are assigned a positive random value (between 1 and 0) multiplied by a constant 10^j where $j = -5$ to render the disturbances small. Finally, numerical simulations are computed using a FORTRAN program with the IMSL subroutine DLSLXG. The central difference formulas with second order accuracy are used for all spatial derivatives and the time derivatives are discretized using Crank-Nicolson method with second order accuracy. In summary, the main steps for the computational procedure are as follows:

1. Initial guesses for U and $\Im$ are generated numerically from a FORTRAN program with the IMSL subroutine RANDOM_NUMBER and, then, multiplied by a constant 10^{-5}.

2. U and $\Im$ at $R = 0$ and $R = 1$ are set to satisfy the conditions (3.13) - (3.17).

3. The basic temperature field is computed.

4. The random force term is generated numerically under the condition that a Gaussian distribution with a vanishing mean and the relation (3.12) for its variance are satisfied.

5. The discretized forms of the time evolution equations, (3.8) and (3.9), are solved using the IMSL subroutine DLSLXG.

6. Evaluate the ratio of the disturbance kinetic energy to its initial value. If it is equal to or greater than 1000, stop. The time at this instant is defined as the onset time of Marangoni instability of an evaporating droplet. Otherwise advance in time and repeat from step 3.

7. Generate N ($N = 5$) times of the same simulations and then calculate the mean average of the onset time from this approximate ensemble.

3.2 RESULTS AND DISCUSSIONS

The stability conditions are investigated for an evaporating octane droplet at two different initial temperatures. The values of the physical properties of octane are referred to the book edited by Dauber & Danner [14]. The evaluation of the physical properties of a gas mixture is provided in Appendix C. Random perturbations are imposed continually during the entire time period of interest. The growth curve of the disturbance kinetic energy is examined to determine the onset time of instability.

Calculations have been made for $Ma = 100,\ 200,\ 300,\ 400,\ 500,\ 600,\ 800,\ 1000,\ 1500,\ 2000, \ldots\ 4000$ with $T_0 = 293K,\ 353K$. For each of the selected Marangoni numbers, the growth of the disturbance kinetic energy, E_{kin}, is calculated for different values of wave number l; that particular value of l with greatest growth of E_{kin} is defined as the critical wave number. For all the cases calculated, the growth rate of the disturbance kinetic energy presents a maximum with respect to the wave number. As an example, the disturbance kinetic energy, E_{kin}, as a function of the wave number, for $T_0 = 293K$, $Ma = 800$, and $\tau = 0.09$, is shown in figure 3.1. As indicated in that figure, the critical wave number is equal to 3. The critical wave numbers for all the cases calculated are summarized in tables 3.1 & 3.2 and are shown in figure 3.2.

The evolution of the kinetic energy of the disturbances at the critical wave numbers for several cases considered are shown in figure 3.3. As energy is being extracted from the basic flow to the perturbed flow, the disturbance kinetic energy grows continually. The time at which the ratio of the disturbance kinetic energy is equal to or greater than 1000 times of its initial value are listed in tables 3.1 & 3.2. These are also presented graphically in figure 3.4.

It needs to be noted that the amplitudes of the initially perturbed velocity components are of the order 10^{-5} (referred to section 3.1). After attaining a thousand-fold increase, the disturbance kinetic energy is of order 10^{-7} and the perturbed velocity components are of order 10^{-3}. The validity of the linearized theory is still ascertained.

As an example, the critical Marangoni numbers for an an evaporating octane droplet at an initial temperature of $293\,K$ and $353\,K$ are calculated. The results indicate that the critical Marangoni number is 190 for that with an initial temperature equal to $293\,K$ and 440 for $353\,K$. The critical wave number are both equal to 1. The evolutions of the disturbance kinetic energy at the critical state for $T_0 = 293\,K$ are shown in figure 3.5. For the case with a subcritical Marangoni number, the disturbances decay finally.

From these results a clear picture of the flow instability is displayed. For an evaporating octane droplet, if the Marangoni number is subcritial, any random perturbation present during the entire time of interest decays steadily. When Marangoni number is increased beyond the critical value, there exists an onset time beyond which the disturbances grow and a new flow pattern becomes observable finally. The lower the supercritical Marangoni number is, the longer it takes for the disturbances to grow into an observable flow pattern.

The onset time for Marangoni instability of an evaporating droplet has been studied by Ha using the quasi-steady approach [26] and the energy method [28], respectively. Moreover, the same problem was then solved by Chou [10] using the initial-value technique. Hence, a comparison between these available mathematical models can be made and possible suggestions might be provided.

For a quasi-steady analysis, the instantaneous temperature profile at a certain instant of interest is frozen first and then the growth of the disturbances are calculated. With the energy method, the variational technique is used to obtain the sufficient

condition for stability. By using the initial-value technique, the initial values of the perturbed fields have to be assumed, and the growth characteristics of certain flow properties are then examined to determine the onset time of instability. The onset of the instability and the corresponding critical wave number calculated by these three different methods are shown in figures 3.2 and 3.4 together with the data from the present study.

Results predicted by the random forcing theory and the initial-value technique are about the same. With the continually imposed disturbances, the onset of instability as predicted by the random forcing theory occurs earlier than that predicted by the initial-value technique. However, the quasi-steady approach which over-estimates the growth rate of the disturbances [47] predicted the earliest occurrence of the instability. Furthermore, the critical wave number obtained by the quasi-steady approach and that by the random forcing theory are not consistent. One possible reason for this discrepancy is that, in the quasi-steady approach, the evolution of the disturbances coupled with the transient basic flow is not considered and the disturbances which grow first are not necessary the ones which grow fastest eventually. With the energy method, Ha [28] obtained the sufficient condition for stability. However, similar trends for the onset of Marangoni instability of an evaporating octane droplet have been predicted by all these different theoretical approaches. The results all indicate that the higher the Marangoni number is, the sooner the droplet becomes unstable due to a greater driving potential for instability. Moreover, the critical Marangoni number increases with the initial temperature, i.e. the droplet with a higher initial temperature seems to be more stable.

As required, an desirable theoretical approach for investigating the behaviour of a system is the one which can simulate those of the laboratory experiments. Due to the lack of available experimental data for comparison, it is difficult to suggest the appropriate instability criterion for the present case. However, the random forcing theory taking into account the random nature of the disturbances observed in experiments might have a big advantage in simulating the realistic onset behaviour of instability of a time dependent flow while the quasi-steady approach could usually provide a clear and direct understanding of the physical mechanism of the onset of instability [28].

Chapter 4

Conclusions and Future Work

4.1 THEORETICAL ANALYSIS OF MARANGONI INSTABILITY OF AN EVAPORATING DROPLET BY RANDOM FORCING THEORY

In this study the stability of an evaporating octane droplet has been examined by random forcing theory. A comparison of the present results with previous theoretical calculations is made. Stability theories usually consider the fate of disturbances imposed at an initial instant while, in random forcing theory, unknown disturbances are imposed continually during the entire time period of calculation (a realistic phenomenon observed in experiments). Similar trends are obtained with different methods. A higher Marangoni number, indicating a greater driving potential for the interfacial convection, is conducive to the onset of instability. The critical Marangoni number increases with the droplet initial temperature. Due to the lack of available experimental results, it is not easy to determine which method is a desirable theoretical approach for investigating such an instability problem but each of them has its own merit in explaining the related instability phenomenon of an evaporating octane droplet.

4.2 RECOMMENDATIONS FOR FUTURE WORK

4.2.1 Effect of moving boundary

During the evaporation process, the position of the free surface is subject to a certain change due to boundary regression. Although the time scale for the interface

regression is, in general, about one order larger than the heat diffusion time scale of the liquid phase, the effect of boundary regression may become significant to the flow instability of a highly volatile liquid or when the initial temperature is close enough to its boiling point. A modified model is then needed to incorporate appropriately the surface regression effect.

4.2.2 Effect of nonlinear interaction

The time evolution equations (3.8) and (3.9), derived in the present study are, strictly speaking, valid only for small fluctuations. However, the approximations involved would become invalid as the Marangoni number approaches its critical value. It is, therefore, of interest, to supplement the linear fluctuation theory with the nonlinear effects. Generally, the convolution sums resulting from nonlinear terms will appear in the time evolution equations and special numerical method has to be used to evaluate them.

Bibliography

[1] Aharon, I. and B.D. Shaw 1996 Marangoni instability of bi-component droplet gasification. *Phys. Fluids*, **8**, 1820-1827.

[2] Benguria, R.D. and M.C. Depassier 1987 Oscillatory instabilities in the Rayleigh-Benard problem with a free surface. *Phys. Fluids*, **30**, 1678-1682.

[3] Benguria, R.D. and M.C. Depassier 1989 On the linear stability theory of Benard-Marangoni convection. *Phys. Fluids A*, **1**, 1123-1127.

[4] Blair, L.M. and J.A. Quinn 1969 The onset of cellular convection in a fluid layer with time-dependent density gradients. *J. Fluid Mech.*, **36**, 385-400.

[5] Brian, P. L. T. and J. R. Ross 1972 The effect of gibbs adsorption on Marangoni instability in penetration mass transfer. *A.I.Ch.E. J.*, **18**, 582-591.

[6] Busse, F.H. and R.M. Clever 1979 Instabilities of convection rolls in a fluid of moderate Prandtl number. *J. Fluid Mech.*, **91**, 319-335.

[7] Busse, F.H. and J.A. Whitehead 1974 Oscillatory and collective instabilities in large Prandtl number convection. *J. Fluid Mech.*, **66**, 67-79.

[8] Chen, D.F. and R.P. Kirchner 1971 Stability of time-dependent rotational Couette flow Part 2. Stability analysis. *J. Fluid Mech.*, **48**, 365-384.

[9] Chen, J.C., G.P. Neitzel, and D.F. Jankowski 1987 Numerical experiments on the stability of unsteady circular Couette flow with random forcing. *Phys. Fluids*, **30**, 1250-1258.

[10] Chou, S.Y. 2001 The analysis of Marangoni instability of an evaporating droplet by amplification method. M.S. Thesis, Department of Mechanical Engineering, National Taiwan University.

[11] Cloot, A. and G. Lebon 1990 Marangoni convection in a rotating spherical geometry. *Phys. Fluids A*, **2**, 525-529.

[12] Cloot, A. and G. Lebon 1990 Surface deformation effect on Marangoni convection in a spherical shell. *Microgravity sci. technol.*, **3**, 44-46.

[13] Cooper, E.R., D.F. Jankowski, G.P. Neitzel, and T.H. Squire 1985 Experiments on the onset of instability in unsteady circular Couette flow.*J. Fluid Mech.*, **161**, 97-113.

[14] Dauber, T. E. and R. P. Danner 1985 Data Compilation Tables of properties of pure compounds, New York.

[15] Davis, S. H. 1969 Buoyancy-surface tension instability by the method of energy. *J. Fluid Mech.*, **39**, 347-359.

[16] Davis, S. H. and C. von Derczek 1973 A reformulation of energy stability theory. *Arch. Ration. Mech. Anal.*, **52**, 122-117.

[17] Davis, S. H. and G. M. Homsy 1980 Energy stability theory for free-surface problems: buoyancy-thermocapillary layers. *J. Fluid Mech.*, **98**, 527-553.

[18] Dijkstra, H.A. and A.I. van de Vooren 1973 Initial flow development due to Marangoni convection in a mass transfer system. *Int. J. Heat Mass Transfer*, **28**, 2315-2322.

[19] Eagles, P.M. Development of Taylor-Couette flow on an intermediate timescale.*Proc. Roy. Soc. Lond. A*, **398**, 289-305.

[20] Edwards, D. K., V. E. Denny and A. F. Mills 1973 Transfer Process, McGraw-Hill, p. 240.

[21] Foster, T.D. 1965 Stability of a homogeneous fluid cooled uniformly from above. *Phys. Fluids, 8*, 1249-1257.

[22] Foster, T.D. 1969 Onset of manifest convection in a layer of fluid with a time-dependent temperature profile. *Phys. Fluids*, **12**, 2482-2487.

[23] Graham, R. 1974 Hydrodynamic fluctuations near the convective instability. *Phys. Rev. A*, **10**, 1762-1784.

[24] Gresho, P.M. and r.L Sani, 1971 The stability of a fluid layer subjected to a step change in temperature: transient vs. frozen time analysis. *Int. J. Heat Mass Transfer*, 14, 207-221.

[25] Gumerman, R. J. and G. M. Homsy 1975 The stability of uniformly accelerated flows with application to convection driven by surface tension. *J. Fluid Mech.*, **68**, 191-207.

[26] Ha, V. M. 1998 The analysis of Marangoni instability of evaporating liquid. Ph.D. Dissertation, Department of Mechanical Engineering, National Taiwan University.

[27] Ha, V. M. and C. L. Lai The onset of stationary Marangoni instability of an evaporating droplet. Accepted for publication in Proceedings A, the Royal Society.

[28] Ha, V.M. 2000 Theoretical analysis of Marangoni instability of an evaporating droplet by energy method. NSC89-2811-E002-0007.

[29] Hoefsloot, H.C.J. and H.W. Hoogstraten 1989 Marangoni instability in spherical shells. *Appl. microgravity tech.*, **2**, 106-108.

[30] Hoefsloot, H.C.J., H.W. Hoogstraten, and L.P.B.M. Janssen 1990 Marangoni instability in a liquid layer confined between two concentric spherical surfaces under zero-gravity conditions. *Applied Scientific Research*, **47**, 357-377.

[31] Hoefsloot, H.C.J., H.W. Hoogstraten, L.P.B.M. Janssen, and J.W. Knobbe 1992 Growth factors for Marangoni instability in a spherical liquid layer under zero-gravity conditions. *Applied Scientific Research*, **49**, 161-173.

[32] Homsy, G. M. 1973 Global stability of time-dependent flows: impulsively heated or cooled fluid layers. *J. Fluid Mech.*, **60**, 129-139.

[33] Homsy, G. M. 1974 Global stability of time-dependent flows. Part2. Modulated fluid layers. *J. Fluid Mech.*, **62**, 387-403.

[34] Horne, R.N. 1979 Three-dimensional natural convection in a confined porous medium heated from below. *J. Fluid Mech.*, **92**, 751-766.

[35] Hubbard, G. L., V. E. Denny and A. F. Mills 1974 Droplet evaporation: Effects of transients and variable properties. *Int. J. Heat Mass Transfer*, **18**, 1003-1008.

[36] Jhaveri, B.S. and G.M. Homsy 1980 Randomly forced Rayleigh-Benard convection. *J. Fluid Mech.*, **98**, 329-348.

[37] Jhaveri, B.S. and G.M. Homsy 1982 The onset of convection in fluid layers heated rapidly in a time-dependent manner. *J. Fluid Mech.*, **114**, 251-260.

[38] Joseph, D. D. 1965 On the stability of the Boussinesq equations. *Arch. Rational Mech. Anal.*, **20**, 59-71.

[39] Joseph, D. D. 1966 Nonlinear stability of the Boussinesq equations by the method of energy. Arch. Rational Mech. Anal., **22**, 163-184.

[40] Joseph, D. D. and C. C. Shir 1966 Subcritical convective instability. *J. Fluid Mech.*, **26**, 753-768.

[41] Joseph, D. D. and C. C. Shir 1966 Subcritical convective instability. *J. Fluid Mech.*, **26**, 769-777.

[42] Kim, K.H. and M.U. Kim 1985 Effect of time-dependent heating on the onset of Rayleigh-Benard convection. *J. Phys. Soc. Jap.*, **54**, 933-941.

[43] Kim, K.H. and M.U. Kim 1986 The onset of natural convection in a fluid layer suddenly heated from below. *Int. J. Heat Mass Transfer*, **29**, 193-201.

[44] Landau, L.D. and E.M. Lifshitz 1959 Fluid Mechanics. Pergamon Press, New York.

[45] Lebon, G., P.C. Dauby, and A. Cloot 1992 Some problem raised by Marangoni instability in spherical geometry. In *Microgravity Fluid Dynamics* (ed. H.J. Rath), Springer, 71-79.

[46] Ludwig, D. Persistence of dynamical systems under random perturbations. *SIAM Review*, **17**, 605-640.

[47] Maher, E.G., R.S. Schechter, and E.H. Wissler 1968 Stability of a fluid layer with time-dependent density gradients. *Phys. Fluids*, **11**, 1901-1912.

[48] Maher, E.G. and R.S. Schechter 1970 The stability of a fluid layer with gas absorption. *Chem. Engng Sci.*, **25**, 955-968.

[49] Mason, E. A. and L. Monchick 1962 Transport properties of polar-gas mixtures. *J. Chem. Phys.*, **36**, 2746-2757.

[50] McTaggart, C. L. 1984 On the stabilizing effect of surface films in Benard convection. *PCH Physicochem. Hydrodyn.*, **5**, 321-331.

[51] Neitzel, G. P. 1982 Onset of convection in impulsively heated or cooled fluid layers. *Phys. Fluids*, **25**, 210-211.

[52] Neitzel, G.P. 1982 Stability of circular Couette flow with variable inner cylinder speed. *J. Fluid Mech.*, **123**, 43-57.

[53] Nielsen, R.C. and R.H. Sabersky 1973 Transient heat transfer in Benard convection. *Int. J. Heat Mass Transfer*, **16**, 2407-2420.

[54] Pearson, J. R. A. 1958 On convection cells induced by surface tension. *J. Fluid Mech.*, **4**, 489-500.

[55] Perez-Garcia, C. and G. Carneiro 1991 Linear stability analysis of Benard-Marangoni convection in fluids with a deformable free surface. *Phys. Fluids A*, **3**, 292-298.

[56] Pirotte, O. and G. Lebon 1988 Surface-tension driven instability in spherical shells. *Appl. microgravity tech.*, **1**, 175-179.

[57] Reid, R. C., Prausnitz, J. M. & Poling, B. E. 1987 The properties of gases and liuqids, McGraw-Hill.

[58] Renardy, Y. and M. Renardy 1985 Perturbation analysis of steady and oscillatory onset in a Benard problem with two similar liquids. *Phys. Fluids*, **28**, 2699-2708.

[59] Renardy, Y. 1986 Interfacial stability in a two-layer Benard problem. *Phys. Fluids*, **29**, 358-363.

[60] Serin, J. 1959 On the stability of viscous fluid motions. *Arch. rat. Mech. Anal.*, **3**, 1-13.

[61] Smith, K. A. 1966 On convective instability induced by surface-tension gradients. *J. Fluid Mech.*, **24**, 401-414.

[62] Sorensen, T. S., M. Hennenberg, A. Steinchen and A. Sanfeld 1975 Chemical and hydrodynamical analysis of stability of a spherical interface. *J. Colloid interface Sci.*, **56**, 191-205.

[63] Sternling, C. V. and L. E. Scriven 1959 Interfacial turbulence: hydrodynamic instability and the Marangoni effect. *A.I.Ch.E. J.*, **5**, 514-523.

[64] Straus, J.M. and G. Schubert 1979 Three-dimensional convection in a cubic box of fluid-saturated porous material. *J. Fluid Mech.*, **91**, 155-165.

[65] Takashima, M. 1970 Nature of the neutral state in convective instability induced by surface tension and buoyancy. *J. Phys. Soc. Japan*, **28**, 810.

[66] Takashima, M. 1981 Surface tension driven instability in a horizontal liquid layer with a deformable free surface. II. Overstability. *J. Phys. Soc. Japan*, **50**, 2715-2756.

[67] Vidal, A. and A. Acrivos 1968 Effect of nonlinear temperature profiles on the onset of convection driven by surface tension gradients. *I&EC Fundamentals.* **7**, 53-58.

[68] Wahal, S. and A. Bose 1988 Rayleigh-Benard and interfacial instabilities in two immiscible liquid layers. *Phys. Fluids*, **31**, 3502-3510.

[69] Wilson, S.K. 1994 The onset of steady Marangoni convection in a spherical geometry. *J. Eng. Math.*, **28**, 427-445.

[70] Zaitsev, V.M. and M.I. Shliomis 1970 Hydrodynamic fluctuations near the convection threshold. *Sov. Phys., J. Exp. Theor. Phys.*, **32**, 866-870.

[71] Zeren, R. W. and W. C. Reynolds 1972 Thermal instabilities in two-fluid horizontal layers. *J. Fluid Mech.*, **53**, 305-327.

Appendix A

Derivation of the condition of tangential stress balance at the free surface

At the free surface, the condition of tangential stress balance (equation (3.1)), as derived in Chapter 3, is obtained from the following equations:

$$R\frac{\partial}{\partial R}(\frac{u'_\theta}{R}) + \frac{1}{R}\frac{\partial u'_R}{\partial \theta} = -\frac{Ma}{R}\frac{\partial T'}{\partial \theta}, \tag{2.49}$$

$$\frac{1}{R\sin\theta}\frac{\partial u'_R}{\partial \phi} + R\frac{\partial}{\partial R}(\frac{u'_\phi}{R}) = -\frac{Ma}{R\sin\theta}\frac{\partial T'}{\partial \phi}. \tag{2.50}$$

Applying the operator $[\frac{1}{\sin\theta}(\frac{\partial}{\partial\theta}\sin\theta)]$ to equation (2.49) and the operator $[\frac{1}{\sin^2\theta}\frac{\partial}{\partial\phi}]$ to equation (2.50), the summation of these two resultant equations leads to

$$\begin{aligned} R\frac{\partial}{\partial R}[\frac{1}{R\sin\theta}\frac{\partial}{\partial\theta}(\sin\theta u'_\theta) + \frac{1}{R\sin\theta}\frac{\partial u'_\phi}{\partial\phi}] + [\frac{1}{R\sin\theta}\frac{\partial}{\partial\theta}(\sin\theta\frac{\partial}{\partial\theta}) + \frac{1}{R\sin^2\theta}\frac{\partial^2}{\partial\phi^2}]u'_R \\ = -\frac{Ma}{R}[\frac{1}{\sin\theta}\frac{\partial}{\partial\theta}(\sin\theta\frac{\partial}{\partial\theta}) + \frac{1}{\sin^2\theta}\frac{\partial^2}{\partial\phi^2}]\Phi. \end{aligned} \tag{A.1}$$

With the aid of the continuity equation (2.38) and the definition of operator L^2 (see equation (3.2)), a new form of the balance of tangential stress is then derived as follows:

$$\frac{\partial^2}{\partial R^2}(Ru'_R) - \frac{(2+L^2)(Ru'_R)}{R^2} = \frac{Ma}{R}L^2T'. \tag{3.1}$$

Appendix B

Derivation of the Perturbed R-Momentum Equation

The momentum equation (3.4) in terms of the radial component of the perturbed velocity (u'_R) can be derived as follows.

First, the pressure term of equation (2.39) is eliminated by taking curl of the whole equation. The vorticity equation becomes

$$(\nabla^2 - \frac{1}{Pr}\frac{\partial}{\partial \tau})\,\vec{\Omega}' = -\nabla \times \nabla \cdot \mathbf{S}', \tag{B.1}$$

where $\vec{\Omega}$ is the vorticity. Then, taking curl of this equation again, it leads to

$$[\nabla^2 - \frac{1}{Pr}\frac{\partial}{\partial \tau}]\nabla^2 \vec{V}' = \nabla \times \nabla \times \nabla \cdot \mathbf{S}'. \tag{B.2}$$

With the aid of the continuity equation (2.38), it can be verified that

$$\vec{R} \cdot \nabla^2 \vec{V}' = \nabla^2(\vec{R} \cdot \vec{V}'). \tag{B.3}$$

Therefore, by taking inner product of equation (B.2) with $\vec{R}$ and using relation (B.3), the perturbed momentum equation in terms of u'_R can then be derived, i.e.,

$$\nabla^2[\nabla^2 - \frac{1}{Pr}\frac{\partial}{\partial \tau}](Ru'_R) = \mathbf{F}. \tag{3.4}$$

where $\mathbf{F} = \vec{R} \cdot \nabla \times \nabla \times \nabla \cdot \mathbf{S}'$.

Appendix C

Evaluation of physical properties of a gas mixture

Values of the physical properties of octane are referred to Dauber & Danner [14]. The diffusivity of component 1 in mixture 1 and 2 (D_{12}) can be calculated by the following equation [57]:

$$D_{12} = \frac{0.001858T^{3/2}[(M_1 + M_2)/M_1M_2]^{1/2}}{p\sigma_{12}^2\Omega_D}, \tag{C.1}$$

where T and p are the temperature and total pressure of the mixture, respectively. M_1 and M_2 represent the molecular weights of these two components involved. The collision integral for mass diffusion Ω_D is a function of kT/ϵ_{12}, where k is the Boltzmann constant. The Lennard-Jones force constants σ_{12} and ϵ_{12} must be obtained from the empirical relations

$$\sigma_{12} = \frac{1}{2}(\sigma_1 + \sigma_2), \tag{C.2}$$

$$\epsilon_{12} = \sqrt{\epsilon_1\epsilon_2}, \tag{C.3}$$

where σ is the collision diameter and ϵ is the maximum energy of attraction between a pair of molecules, for each individual species.

To accommodate the variation of the gas phase properties, a simple 1/3 rule [35] is used. According to that rule, the reference temperature is evaluated as

$$T_{ref} = T_s + \frac{1}{3}(T_0 - T_s), \tag{C.4}$$

and the reference mole fraction of liquid vapor, $m_{v,ref}$, used for the evaluation of the mixture properties is expressed as

$$m_{v,ref} = m_{v,s} + \frac{1}{3}(m_{v,\infty} - m_{v,s}), \tag{C.5}$$

where $m_{v,s}$ is the mole fraction of liquid vapor at the free surface. Moreover, the Mason-Monchik mixture rule [49] is used for the evaluation of the mixture viscosity and the Wilke rule is used [20] for the mixture thermal conductivity. The thermodynamic properties and molecular weights of the mixture are calculated by assuming an ideal gas mixture.

process	timescale	timescale w.r.t. r_0^2/α_l
gas phase flow	r_0/A_0	$\frac{\alpha_l}{A_0 r_0} = \frac{1}{RePr_l}\frac{\mu_l}{\mu_g}\frac{\rho_g}{\rho_l} \sim (10^{-2} \sim 10^{-1})$
transport in gas phase		
a) diffusion of momentum	r_0^2/ν_g	$\frac{\alpha_l}{\nu_g} = \frac{\alpha_l}{\alpha_g}\frac{1}{Pr_g} \sim 10^{-2}$
b) diffusion of heat	r_0^2/α_g	$\frac{\alpha_l}{\alpha_g} \sim 10^{-2}$
c) diffusion of mass	r_0^2/D_g	$\frac{\alpha_l}{D_g} = \frac{\alpha_l}{\alpha_g}Le \sim 10^{-2}$
transport in liquid phase		
a) diffusion of momentum	r_0^2/ν_l	$\frac{\alpha_l}{\nu_l} = \frac{1}{Pr_l} \sim (10^{-1} \sim 1)$
b) diffusion of heat	r_0^2/α_l	1
droplet regression	$\frac{r_0}{\dot{r}_0} \simeq \frac{r_0\rho_l}{A_0\rho_g}$	$\frac{\alpha_l}{A_0 r_0}\frac{\rho_l}{\rho_g} = \frac{1}{RePr_l}\frac{\mu_l}{\mu_g} \sim (10 \sim 10^2)$

Table 2.1 Comparison of the various time scales during evaporation; based on data for octane and heptane from Daubert & Danner (1985): $\rho_l/\rho_g \sim O(10^3)$, $Pr_l \sim O(1 \sim 10)$, $\alpha_l/\alpha_g \sim O(10^{-2})$, $\mu_l/\mu_g \sim O(10^2)$, $Pr_g \sim 1$, $Le \sim 1$, $Re = A_0 r_0/\nu_g$ = **radial Reynold number** $\sim O(1)$, A_0 = **evaporating velocity at free surface.**

Ma	critical wave number l_c	Onset time τ
100	-	-
200	1	0.8402
300	1	0.4225
400	2	0.2569
500	2	0.1854
600	3	0.1417
800	3	0.0939
1000	4	0.0680
1500	5	0.0378
2000	6	0.0242
2500	7	0.0168
3000	8	0.0121
3500	9	0.0090
4000	10	0.0066

Table 3.1 The onset time and the corresponding critical wave number at the occurrence of the Marangoni instability of an octane droplet with $T_0 = 293\,K$.

Ma	critical wave number l_c	Onset time τ
100	-	-
200	-	-
300	-	-
400	-	-
500	1	0.5073
600	2	0.2584
800	3	0.1423
1000	3	0.0965
1500	5	0.0493
2000	6	0.0302
2500	7	0.0205
3000	8	0.0146
3500	8	0.0106
4000	9	0.0078

Table 3.2 The onset time and the corresponding critical wave number at the occurrence of the Marangoni instability of an octane droplet with $T_0 = 353$.

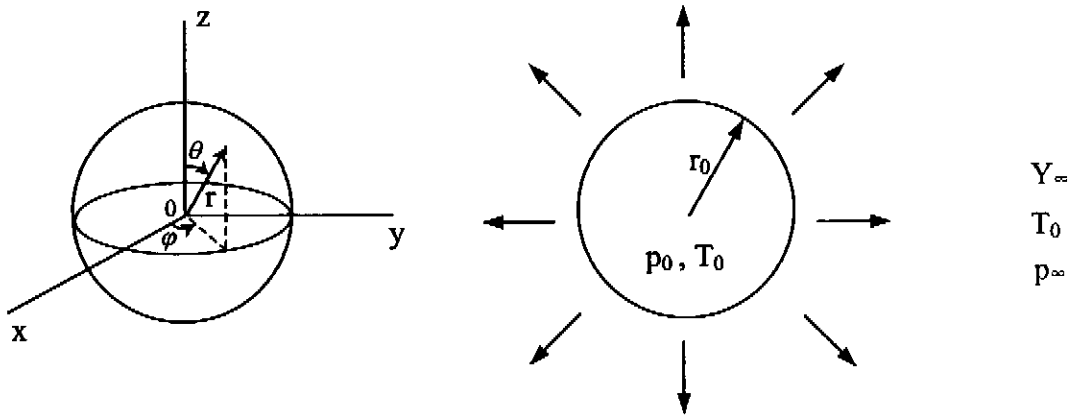

Figure 2.1 The schematic diagram of the physical model and coordinate system for an evaporating liquid droplet.

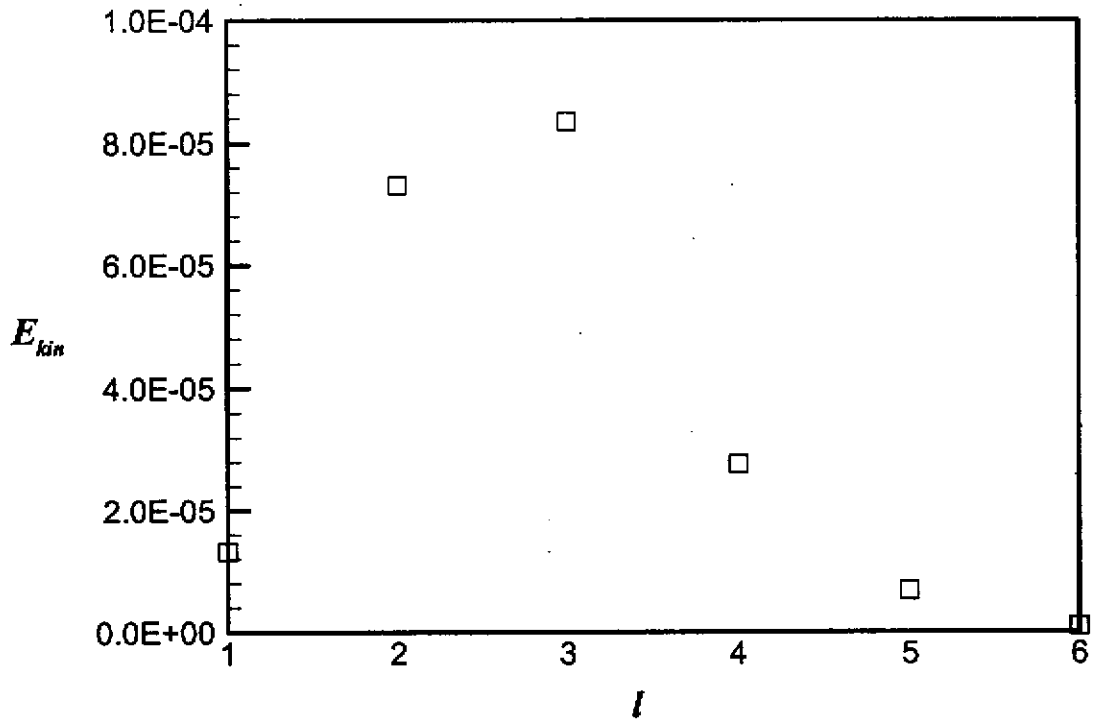

Figure 3.1 Determination of the critical wave number for $T_0 = 293$ K, Ma = 800, and $\tau = 0.09$.

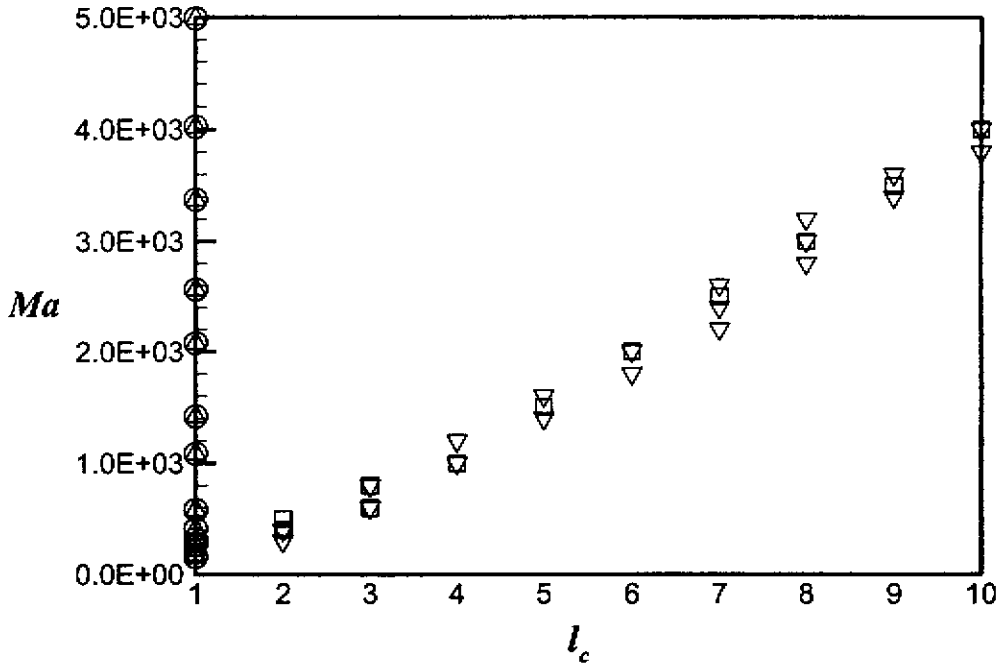

Figure 3.2a The critical wave number for different Marangoni numbers at $T_0 = 293$ K; □, random forcing theory; ∇, initial-value technique; Δ, energy method; o, quasi-steady analysis.

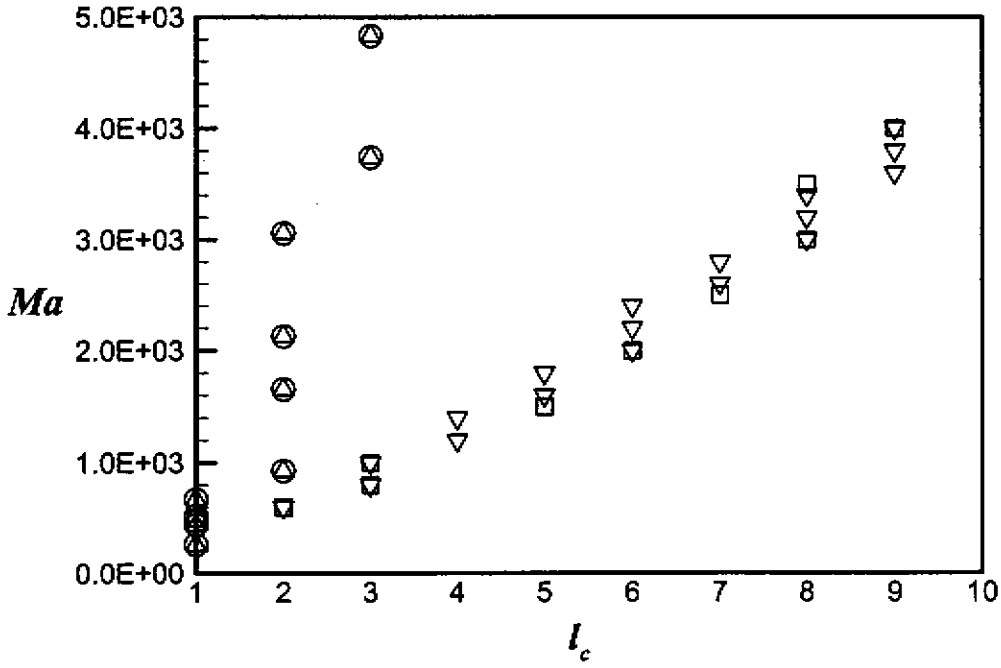

Figure 3.2b The critical wave number for different Marangoni numbers at $T_0 = 353$ K; □, random forcing theory; ∇, initial-value technique; Δ, energy method; o, quasi-steady analysis.

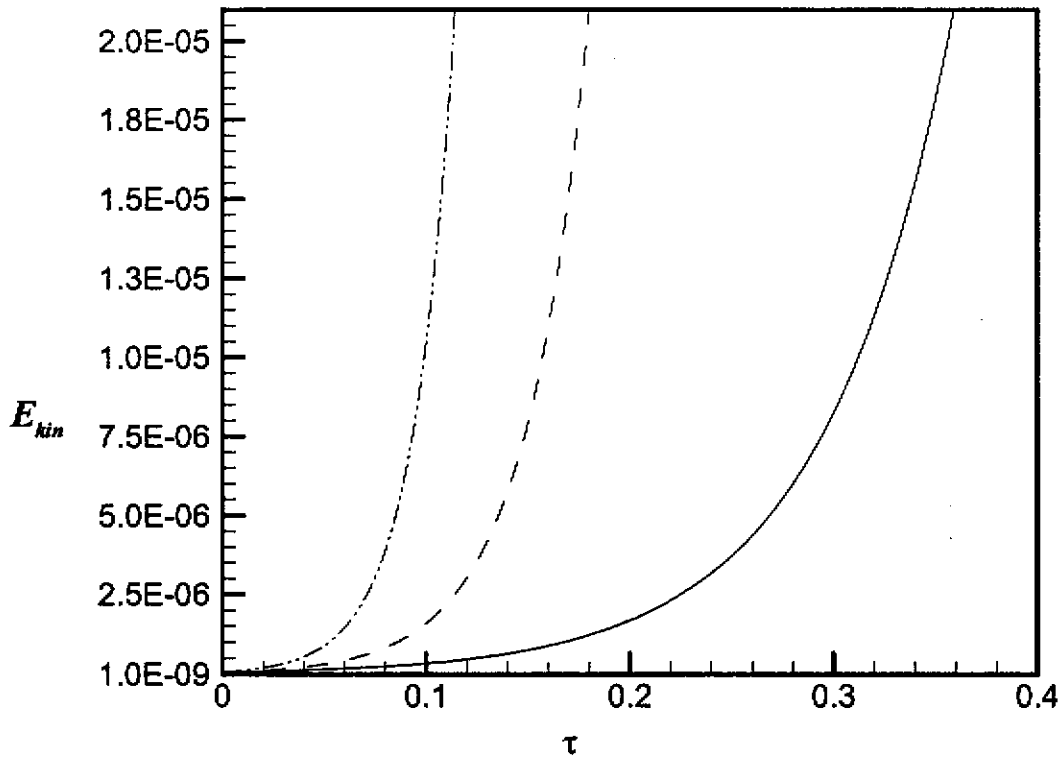

Figure 3.3 The evolution of the disturbance kinetic energy at the critical wave numbers for different Marangoni numbers with T_0 = 293 K; ———, Ma = 200; ----------, Ma = 400; — -- — --, Ma = 600.

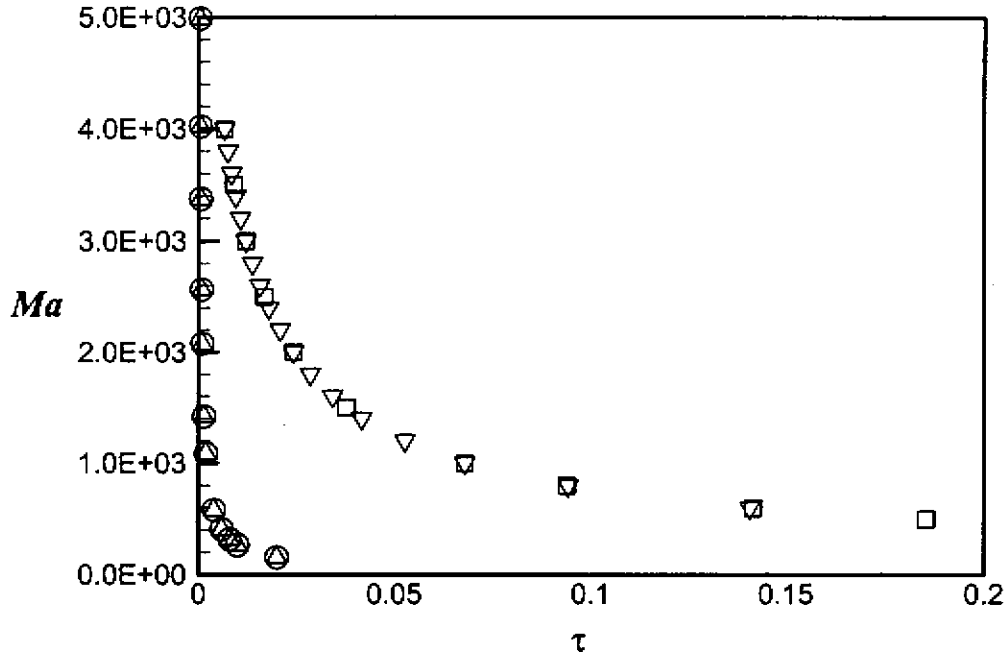

Figure 3.4a The onset time of the Marangoni instability for different Marangoni numbers at $T_0 = 293$ K; □, random forcing theory; ∇, initial-value technique; Δ, energy method; o, quasi-steady analysis.

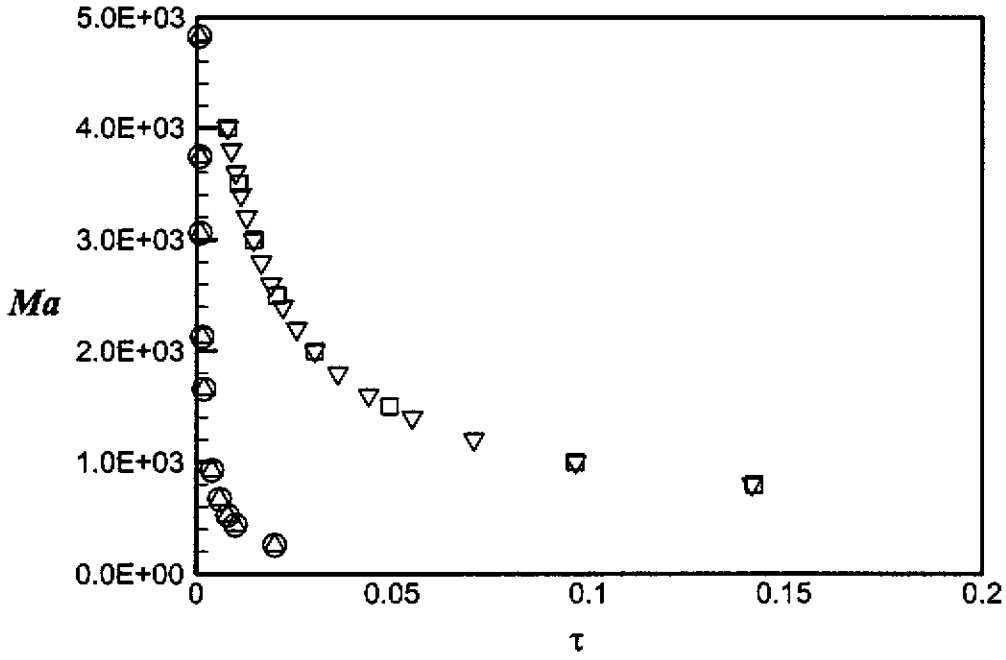

Figure 3.4b The onset time of the Marangoni instability for different Marangoni numbers at $T_0 = 353$ K; □, random forcing theory; ∇, initial-value technique; Δ, energy method; o, quasi-steady analysis.

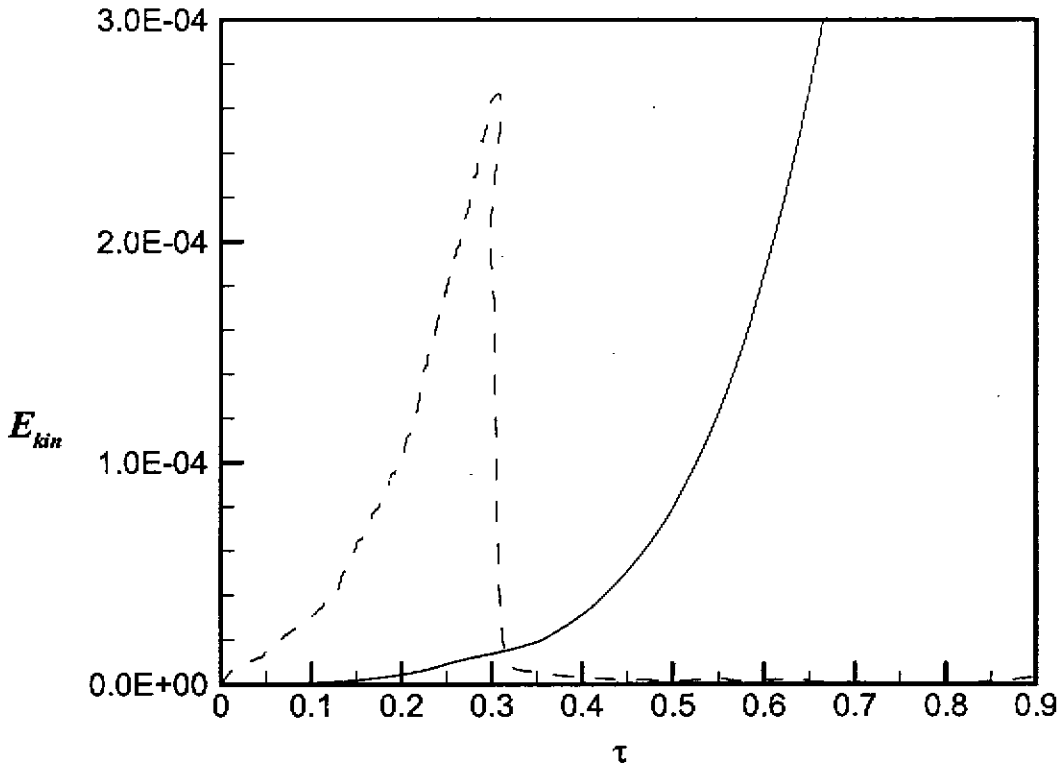

Figure 3.5 The evolution of the disturbance kinetic energy at the critical and the subcritical Marangoni number for $T_0 = 293$ K; ———, Ma = 190; ---------, Ma=100.